Journal of Magnetic Resonance **155,** 300–306 (2002)
doi:10.1006/jmre.2002.2520, available online at http://www.idealibrary.com on IDEAL®

COMMUNICATIONS

Cogwheel Phase Cycling

Malcolm H. Levitt,* P. K. Madhu,* and Colan E. Hughes†

*Chemistry Department, Southampton University, England SO17 1BJ; and †Physical Chemistry Division, Stockholm University, S-10691 Sweden

E-mail: Malcolm.Levitt@soton.ac.uk

Received November 26, 2001; revised February 5, 2002

A new method for constructing phase cycles is described. The new schemes apply to experiments involving several consecutive coherence transfer steps. The radiofrequency phases of two or more irradiation blocks are incremented simultaneously, as opposed to the traditional "nested" scheme, in which the block phases are incremented independently. In many cases, the "cogwheel" phase cycles achieve the same selectivity as traditional phase cycles, using fewer steps. Significant time savings are achievable in a wide range of NMR experiments.

Key Words: **phase cycling; coherence transfer pathways; cogwheel phase cycles.**

INTRODUCTION

Phase cycling is one of the most important general tools in NMR pulse sequence design. In general, phase cycling involves repetition of an NMR pulse sequence several times, with the same values of the time intervals and rf amplitudes and frequencies, but with variation of one or more radiofrequency phases. The different NMR signals are multiplied by complex phase factors and added together. A properly designed phase cycle allows the selection of well-defined classes of NMR signals, with suppression of undesirable or uninteresting NMR signals, and in some cases, suppression of artifacts arising from instrumental imperfections.

In many experimental situations, the time span of an NMR experiment is determined by the need to complete the phase cycle, rather than the necessity of accumulating sufficient signal. There is therefore a strong motivation for constructing phase cycles of minimal length.

The modern theory of phase cycling was established independently by Bodenhausen *et al.* (*1*) and by Bain (*2*). This theory established the importance of the coherence transfer pathway (CTP), which is defined as the chronological sequence of spin coherence orders giving rise to a particular signal component.

In this paper, we use a modified notation for the rf phases and the coherence transfer orders to make a clearer correspondence with the pulse sequence. Consider the case where a pulse sequence is composed of three independent blocks, A, B, C. The *overall* phases of the different blocks $\{\phi_A, \phi_B, \phi_C\}$ may be varied with respect to each other, but the *relative* phases and timings of pulses within each block are always kept fixed. The complex NMR signal at time t after the end of the pulse sequence may be expressed

$$s(t) = \sum_{\boldsymbol{p}} s_{\boldsymbol{p}}(t), \qquad [1]$$

where $\boldsymbol{p}$ denotes a coherence transfer pathway, $\boldsymbol{p} = \{0, p_{AB}, p_{BC}, -1\}$. Here p_{AB} represents the order of coherences in the interval between the blocks A and B, p_{BC} represents the order of coherences in the interval between the blocks B and C. All pathways originate with order 0, representing a reproducible initial state containing only spin state populations, and terminate with order -1, representing quadrature detection of the free-induction decay and construction of a complex NMR signal (*3, 4*).

Each of the signal components $s_{\boldsymbol{p}}$ has a well-defined dependence on the overall phases $\{\phi_A, \phi_B, \phi_C\}$ of the pulse sequence blocks, and on the signal detection phases, according to

$$s_{\boldsymbol{p}}(t; \phi_A, \phi_B, \phi_C, \phi_{\mathrm{rec}}, \phi_{\mathrm{dig}}) = s_{\boldsymbol{p}}(t; 0, 0 \ldots) \exp\{-\mathrm{i}\Phi(\boldsymbol{p})\}, \qquad [2]$$

where

$$\Phi(\boldsymbol{p}) = \phi_A \Delta p_A + \phi_B \Delta p_B + \phi_C \Delta p_C + \phi_{\mathrm{rec}} + \phi_{\mathrm{dig}}, \qquad [3]$$

where ϕ_{rec} is the radiofrequency receiver reference phase, and ϕ_{dig} is the post-digitization phase shift (*4*). Here $\{\Delta p_A, \Delta p_B, \Delta p_C\}$ are the changes in coherence order induced by the pulse sequence blocks, i.e.,

$$\begin{aligned} \Delta p_A &= p_{AB} - 0 = p_{AB} \\ \Delta p_B &= p_{BC} - p_{AB} \\ \Delta p_C &= -1 - p_{BC}. \end{aligned} \qquad [4]$$

1090-7807/02 $35.00

Suppose that the overall phases are cycled in a series of N steps, i.e., $\{\phi_A, \phi_B, \phi_C, \phi_{\text{rec}}, \phi_{\text{dig}}\}$ take the values $\{\phi_A^{(0)}, \phi_B^{(0)}, \phi_C^{(0)}, \phi_{\text{rec}}^{(0)}, \phi_{\text{dig}}^{(0)}\}$, $\{\phi_A^{(1)}, \phi_B^{(1)}, \phi_C^{(1)}, \phi_{\text{rec}}^{(1)}, \phi_{\text{dig}}^{(1)}\}\ldots$ in successive acquired transients. Denote the phase cycle counter by $m = 0, 1, \ldots N-1$. The pathway phase for transient m is given by

$$\Phi^{(m)}(\boldsymbol{p}) = \phi_A^{(m)}\Delta p_A + \phi_B^{(m)}\Delta p_B + \phi_C^{(m)}\Delta p_C + \phi_{\text{rec}}^{(m)} + \phi_{\text{dig}}^{(m)}. \quad [5]$$

Phase cycles consist of a set of N experiments for which the pathway phase factors $\exp\{-i\Phi^{(m)}(\boldsymbol{p})\}$ constructively interfere for desired signal pathways $\boldsymbol{p} \in \{\boldsymbol{p}^0, \boldsymbol{p}^{0\prime}\ldots\}$, and destructively interfere for undesired signal pathways $\boldsymbol{p} \notin \{\boldsymbol{p}^0, \boldsymbol{p}^{0\prime}\ldots\}$:

$$N^{-1}\sum_{m=0}^{N-1}\exp\{-i\Phi^{(m)}(\boldsymbol{p})\} = \begin{cases} 1 & \text{if } \boldsymbol{p} \in \{\boldsymbol{p}^0, \boldsymbol{p}^{0\prime}\ldots\} \\ 0 & \text{otherwise.} \end{cases} \quad [6]$$

Constructive interference for desired pathways is ensured by selecting the phases so as to satisfy the "master equation"

$$\Phi^{(m)}(\boldsymbol{p}) = \text{constant} \qquad \text{if } \boldsymbol{p} \in \{\boldsymbol{p}^0, \boldsymbol{p}^{0\prime}\ldots\} \quad [7]$$

for all transients m. It is more difficult to ensure complete destructive interference for all undesired pathways. The subject of this communication is to find phase cycles satisfying Eq. [6] with small values of N.

CONVENTIONAL PHASE CYCLING

To make this discussion concrete, consider the pulse sequence for the triple-quantum NMR of spin-3/2 systems sketched in Fig. 1. This consists of three blocks: The first block excites (+3)-quantum coherences starting from a thermal equilibrium state ($p_{AB} = +3$). The second block partially converts these coherences into (+1)-quantum coherences, in order to induce a second-order quadrupolar echo (*5–11*) ($p_{BC} = +1$). The third block consists of a π pulse, which converts the (+1)-quantum coherences into observable (−1)-quantum coherences, in order to obtain pure absorption 2D spectra (*9*). The pulse sequence denoted here consists of the recently developed FAM-RIACT-FAM sequence, which gives particularly high signal intensities (*11, 26*), but the discussion is general for all 3-quantum experiments in spin-3/2 systems.

In this particular experiment, only the single pathway $\boldsymbol{p}^0 = \{0, +3, +1, -1\}$ gives rise to useful high-resolution NMR spectra. Signals from all other pathways should be discarded by the phase cycle. In the case of isolated spins-3/2, only pathways involving coherence orders $-3 \le p \le 3$ need to be considered.

There are different ways of implementing the conventional procedure for constructing phase cycles. For example, all pathways with orders $p_{AB} \neq +3$ may be suppressed by cycling block A in a minimum of 7 steps. The number 7 arises because the order change $\Delta p_A = +3$ should be allowed, while the six adjacent order changes $\Delta p_A = \{+2, +1, 0, -1, -2, -3\}$ should be suppressed. Similarly, all pathways with orders $p_{BC} \neq +1$ may be suppressed by cycling block C in a minimum of 5 steps. The number 5 arises because the order change $\Delta p_C = -2$ should be allowed, while the four adjacent order changes $\Delta p_C = \{+2, +1, 0, -1\}$ should be suppressed. (Five-step cycling automatically suppresses the additional undesired order changes $\Delta p_C = \{-3, -4\}$.) In order to separate these selection rules cleanly, the phases of blocks A and C are cycled in a nested fashion, leading to a 35-step phase cycle, according to

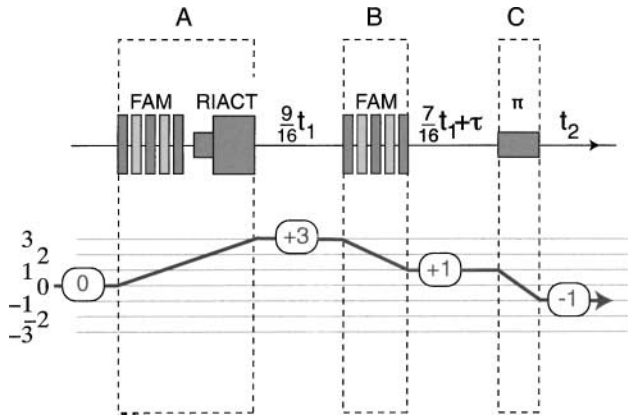

FIG. 1. FAM-RIACT-FAM pulse sequence for triple-quantum MAS of spin-3/2 systems, and its coherence transfer pathway diagram (see Ref. (*11*)). The FAM sequence consists of strong short pulses with phases differing by π radians. The RIACT sequence consists of a selective $\pi/2$ pulse on the central transition followed by one-quarter of a rotor period of strong rf irradiation, phase shifted by $\pi/2$ radians. (+3)-quantum coherences are excited by the initial FAM-RIACT sequence, and converted into central transition (+1)-quantum coherence by the second FAM sequence. The π pulse forms a central transition single-quantum echo which is used to obtain pure absorption 2D spectra. The pulse sequence includes a split-t_1 interval and an echo interval τ. The overall phases of the three blocks A, B, and C, as well as the receiver and digitizer phases ϕ_{rec} and ϕ_{dig}, are cycled to select out signals passing through the desired pathway $\boldsymbol{p}^0 = \{0, +3, +1, -1\}$.

$$\begin{aligned} \phi_A^{(m)} &= \frac{2\pi}{7}m \\ \phi_B^{(m)} &= 0 \\ \phi_C^{(m)} &= \frac{2\pi}{5}\text{floor}\left(\frac{m}{7}\right), \end{aligned} \quad [8]$$

where m is the phase cycle counter, $m = 0, 1, \ldots 34$, and floor(x) is the largest integer which is not greater than x (4). In order to ensure that the signals from the desirable pathway $\boldsymbol{p}^0 = \{0, +3, +1, -1\}$ constructively interfere, the signal detection phases $\phi_{\text{rec}}^{(m)}$ and $\phi_{\text{dig}}^{(m)}$ are adjusted to satisfy the "master equation" (Eq. [7]), for example by choosing the phases such that

$$+3\phi_A^{(m)} - 2\phi_B^{(m)} - 2\phi_C^{(m)} + \phi_{\text{rec}}^{(m)} + \phi_{\text{dig}}^{(m)} = 0. \quad [9]$$

For example, one implementation of the 35-step phase cycle would combine Eq. [8] with the following receiver phase cycle

$$\begin{aligned}\phi_{\mathrm{rec}}^{(m)} &= -3\frac{2\pi}{7}m + 2\frac{2\pi}{5}\mathrm{floor}\left(\frac{m}{2}\right)\\ \phi_{\mathrm{dig}}^{(m)} &= 0.\end{aligned} \qquad [10]$$

If desired, suppression of receiver artifacts could be implemented by super imposing a further layer of phase cycling involving the postdigitization phase shifter.

It is possible to construct nested phase cycles in other ways. For example, block B could be cycled instead of block C. This also leads to 35-step phase cycle. The desired order change over block B is $\Delta p_B = -2$, and the four adjacent changes $\Delta p_B = \{-3, -4, -5, -6\}$ must be suppressed, suggesting a 5-step cycle for block B. This 5-step cycle also suppresses the undesired order changes $\Delta p_B = \{0, -1\}$. As a result, a cycle based on phase variations for blocks A and B also has $7 \times 5 = 35$ steps.

The inescapable conclusion seems to be that the minimal phase cycle for this problem (if receiver artifacts are neglected) is 35 steps.

COGWHEEL PHASE CYCLING

In order to develop a new approach to phase cycling, consider a strategy in which the phases of the pulse sequence blocks are incremented simultaneously, at a defined ratio of angular velocities, like a set of meshing cogwheels.

For example, in the MQ-MAS case discussed above, make an *ansatz* that the phases of blocks A, B, and C are incremented

$$\begin{aligned}\phi_A^{(m)} &= \frac{2\pi\nu_A}{N}m\\ \phi_B^{(m)} &= \frac{2\pi\nu_B}{N}m\\ \phi_C^{(m)} &= \frac{2\pi\nu_C}{N}m,\end{aligned} \qquad [11]$$

where ν_A, ν_B, ν_C are integers called the *winding numbers*, N is the number of steps in the phase cycle, and m is the phase cycle counter, $m = \{0, 1, \ldots N-1\}$. These equations define a N-step phase cycle, with the phase ϕ_A incrementing in steps of $\nu_A \times (2\pi/N)$, the phase ϕ_B incrementing in steps of $\nu_B \times (2\pi/N)$, and the phase ϕ_C incrementing in steps of $\nu_C \times (2\pi/N)$, all at the same time. When the complete cycle of N steps is completed, the phase ϕ_A will have completed ν_A full revolutions, the phase ϕ_B will have completed ν_B full revolutions, and the phase ϕ_C will have completed ν_C full revolutions. The notation used here is borrowed from the symmetry theory of recoupling sequences in solid-state NMR (*12–17*).

The accumulated phase for a general pathway $\boldsymbol{p} = \{0, p_{AB}, p_{BC}, -1\}$ is given by

$$\begin{aligned}\Phi^{(m)}(\boldsymbol{p}) &= \phi_A^{(m)}\Delta p_A + \phi_B^{(m)}\Delta p_B + \phi_C^{(m)}\Delta p_C + \phi_{\mathrm{rec}}^{(m)} + \phi_{\mathrm{dig}}^{(m)}\\ &= \frac{2\pi m}{N}(\nu_A\Delta p_A + \nu_B\Delta p_B + \nu_C\Delta p_C) + \phi_{\mathrm{rec}}^{(m)} + \phi_{\mathrm{dig}}^{(m)}.\end{aligned} \qquad [12]$$

It proves to be convenient to define the *differences* between the winding numbers for adjacent pulse sequence blocks as

$$\begin{aligned}\Delta\nu_{AB} &= \nu_B - \nu_A\\ \Delta\nu_{BC} &= \nu_C - \nu_B.\end{aligned} \qquad [13]$$

The accumulated phase for a general pathway may then be expressed

$$\begin{aligned}\Phi^{(m)}(\boldsymbol{p}) = \frac{2\pi m}{N}\{&-\Delta\nu_{AB}\,p_{AB} - \Delta\nu_{BC}\,p_{BC}\\ &-(\nu_A + \Delta\nu_{AB} + \Delta\nu_{BC})\} + \phi_{\mathrm{rec}}^{(m)} + \phi_{\mathrm{dig}}^{(m)}.\end{aligned} \qquad [14]$$

Note that this equation involves the *absolute* coherence orders $\{p_{AB}, p_{BC} \ldots\}$ between blocks, rather than the *changes* in coherence orders induced by a pulse sequence block.

Now suppose that on each step of the phase cycle, the receiver and digitizer phase are adjusted according to the "master equation" (Eq. [7]) for the desired pathway $\boldsymbol{p}^0$. This ensures that the signals from the desired pathway constructively interfere on each step. Under these conditions we may recast Eq. [14]

$$\Phi^{(m)}(\boldsymbol{p}) = \frac{2\pi m}{N}\left\{-\Delta\nu_{AB}\left(p_{AB} - p_{AB}^0\right) - \Delta\nu_{BC}\left(p_{BC} - p_{BC}^0\right)\right\}, \qquad [15]$$

where p_{AB}^0 is the order of the pathway $\boldsymbol{p}^0$ between blocks A and B, and p_{BC}^0 is the order of the pathway $\boldsymbol{p}^0$ between blocks B and C. The selection rule for this cogwheel cycle is therefore based on the value of the sum

$$\begin{aligned}S(\boldsymbol{p}) = N^{-1}\sum_{m=0}^{N-1}\exp\Bigg\{\mathrm{i}\frac{2\pi m}{N}\big[&\Delta\nu_{AB}\left(p_{AB} - p_{AB}^0\right)\\ &+ \Delta\nu_{BC}\left(p_{BC} - p_{BC}^0\right)\big]\Bigg\}.\end{aligned} \qquad [16]$$

It is easily shown (*4*) that this sum evaluates to

$$S(\boldsymbol{p}) = \begin{cases}1 & \text{if } (\Delta\nu_{AB}\,p_{AB} + \Delta\nu_{BC}\,p_{BC})\\ & \quad = \left(\Delta\nu_{AB}\,p_{AB}^0 + \Delta\nu_{BC}\,p_{BC}^0\right) + N \times \text{integer}\\ 0 & \text{otherwise.}\end{cases} \qquad [17]$$

Equation [17] is the general selection rule for cogwheel phase cycling in the case of three pulse sequence blocks, A, B, and C.

Feasible cogwheel phase cycles may be found by searching for combinations of N, $\Delta\nu_{AB}$, and $\Delta\nu_{BC}$ such that the equality $(\Delta\nu_{AB}p_{AB} + \Delta\nu_{BC}p_{BC}) = (\Delta\nu_{AB}p^0_{AB} + \Delta\nu_{BC}p^0_{BC}) + N \times$ integer is satisfied for all *desired* pathways $\boldsymbol{p} \in \{\mathbf{p}^0, \mathbf{p}^{0'} \ldots\}$, while the same equality is *not* satisfied for all *undesired* pathways.

For example, in the MQ-MAS case discussed above, there is only one desired coherence transfer pathway, namely $\boldsymbol{p}^0 = \{0, +3, +1, -1\}$. Feasible cogwheel phase cycles satisfy

$$(\Delta\nu_{AB}p_{AB} + \Delta\nu_{BC}p_{BC}) \neq (3\Delta\nu_{AB} + \Delta\nu_{BC}) + N \times \text{integer} \quad [18]$$

for all pathways $\boldsymbol{p} \neq \boldsymbol{p}^0$ which start at order 0, terminate at order -1, and which pass through coherence orders satisfying $-3 \leq p_{AB} \leq +3$ and $-3 \leq p_{BC} \leq +3$.

A numerical search shows that the shortest solutions exist for the case $N = 23$. There are 22 such solutions, including $\{N, \Delta\nu_{AB}, \Delta\nu_{BC}\} = \{23, +3, +1\}$, $\{23, 2, -7\}$, $\{23, 1, 8\}$, $\{23, 4, 9\}$, $\{23, 5, -6\}$, $\{23, 7, 10\}$, and their phase-inverted counterparts, $\{23, -3, -1\}$, $\{23, -2, +7\}$, $\{23, -1, -8\}$, $\{23, -4, -9\}$, $\{23, -5, +6\}$, and $\{23, -7, -10\}$. There are also numerous solutions with $N > 23$.

In order to clarify the implementation of a cogwheel phase cycle, consider the solutions with $\{N, \Delta\nu_{AB}, \Delta\nu_{BC}\} = \{23, +3, +1\}$. One implementation may be realized by assuming that the first pulse sequence block has constant phase, i.e., $\nu_A = 0$. From Eq. [13], we get $\nu_B = \Delta\nu_{AB} = +3$ and $\nu_C = \Delta\nu_{BC} + \nu_B = +1 +3 = +4$. The cogwheel phases for the three pulse sequence blocks are therefore

$$\begin{aligned} \phi_A^{(m)} &= 0 \\ \phi_B^{(m)} &= \frac{3 \times 2\pi}{23} m \\ \phi_C^{(m)} &= \frac{4 \times 2\pi}{23} m, \end{aligned} \quad [19]$$

where m is the phase cycle counter, $m = 0, 1, \ldots 22$. The receiver and digitizer phase may be constructed from the master equation for the desired pathway $\boldsymbol{p}^0$ (Eq. [9]), which leads to

$$\begin{aligned} \phi_{\text{rec}}^{(m)} &= \frac{14 \times 2\pi}{23} m \\ \phi_{\text{dig}}^{(m)} &= 0. \end{aligned} \quad [20]$$

This defines a 23-step phase cycle in which the phase of the first pulse sequence block is fixed, the phase of the second pulse sequence block is incremented in steps of $(3/23) \times 360^\circ = 46.96^\circ$, the phase of the third pulse sequence block is incremented in steps of $(4/23) \times 360^\circ = 62.61^\circ$, and the receiver reference phase is incremented in steps of $(14/23) \times 360^\circ = 219.13^\circ$, *all at the same time*. In this paper, we denote this cogwheel cycle by the notation COG23(0, 3, 4; 14).

An equivalent cogwheel cycle is formed by assuming that the second block has constant phase, i.e. $\nu_B = 0$. From Eq. [13], we get $\nu_A = -\Delta\nu_{AB} = -3$ and $\nu_C = +\Delta\nu_{BC} = +1$. We therefore have the following expressions for the phases of the pulse blocks,

$$\begin{aligned} \phi_A^{(m)} &= -\frac{3 \times 2\pi}{23} m \\ \phi_B^{(m)} &= 0 \\ \phi_C^{(m)} &= +\frac{1 \times 2\pi}{23} m. \end{aligned} \quad [21]$$

The master equation Eq. [9] for the pathway $\boldsymbol{p}^0 = \{0, +3, +1, -1\}$ provides the expression for the receiver phase $\phi_{\text{rec}}^{(m)} = ((-3) \times (-3) + (+2) \times (+1)) \times (2\pi m/23) = 11 \times 2\pi m/23$, assuming that the digitizer phase is held at $\phi_{\text{dig}}^{(m)} = 0$. This cogwheel cycle therefore has the notation COG23(-3, 0, $+1$; 11).

Further cogwheel cycles may be constructed by using different solutions for $\{N, \Delta\nu_{AB}, \Delta\nu_{BC}\}$. For example, one implementation of the solution $\{N, \Delta\nu_{AB}, \Delta\nu_{BC}\} = \{23, -3, -1\}$ is the cycle COG23($+3$, 0, -1; -11). Similarly, the solution $\{N, \Delta\nu_{AB}, \Delta\nu_{BC}\} = \{23, 2, -7\}$ may be implemented through the cogwheel cycle COG23(0, 2, -5; -6).

All of these 23-step cogwheel phase cycles have the same selection properties as the conventional 35-step nested phase cycles. Both types of phase cycle suppress all possible coherence transfer pathways in a system of isolated spins-3/2, except for the second-order quadrupolar echo pathway $\{0, +3, +1, -1\}$.

COGWHEEL SELECTION DIAGRAMS

The selection rule in Eq. [18] is readily visualized by using a *cogwheel selection diagram*. Figure 2 shows a cogwheel selection diagram for the set of cycles with $\{N, \Delta\nu_{AB}, \Delta\nu_{BC}\} = \{23, +3, +1\}$. This diagram shows the possible values of $\Delta\nu_{AB}p_{AB} + \Delta\nu_{BC}p_{BC}$, plotted as horizontal "levels." The construction of the levels is split into two steps, with level spacings in a ratio of 3 to 1, to reflect the winding numbers $\Delta\nu_{AB} = +3$ and $\Delta\nu_{BC} = +1$. In the case shown, the coherence orders p_{AB} and p_{BC} take all integer values between -3 and $+3$, so that each of the 7 branches splits into 7 subbranches. The barrier on the right-hand side has holes spaced by 23 units. As may be seen, this is just enough to clearly separate the $\{p_{AB}, p_{BC}\} = \{+3, +1\}$ pathway from all of the others. One can also see that the winding number $\Delta\nu_{AB} = +3$ is just sufficient to separate the desirable $\{p_{AB}, p_{BC}\} = \{+3, +1\}$ pathway from the multiple branches with $p_{AB} = +2$.

The cogwheel selection diagrams are closely related to the space-spin selection diagrams employed in the construction of symmetry-based pulse sequences in solid-state NMR (*12–17*).

The selection diagrams also give some insight into how the cogwheel cycles gain efficiency over the nested phase cycles. Figure 2 shows that many of the undesirable pathways have the same value of $\Delta\nu_{AB}p_{AB} + \Delta\nu_{BC}p_{BC}$, and hence have the same

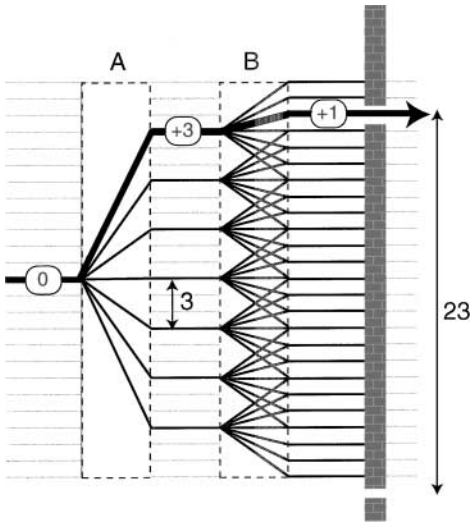

FIG. 2. Cogwheel selection diagram for the 3Q-MAS pulse sequence. The barrier on the right-hand side, with holes separated by 23 units, represents the selection rule for cogwheel phase cycles defined by $\{N, \Delta\nu_{AB}, \Delta\nu_{BC}\} = \{23, +3, +1\}$. The pulse sequence A splits the initial state into a set of pathways with coherence orders running from $p_{AB} = -3$ to $p_{AB} = +3$, each separated by 3 units, according to the winding number difference $\Delta\nu_{AB} = +3$. The pulse sequence B splits each of these pathways into a new set of subpathways separated by 1 unit, according to the winding number difference $\Delta\nu_{BC} = +1$. The desired pathway $\{p_{AB}, p_{BC}\} = \{+3, +1\}$ is indicated by a bold line. Note that the desired pathway terminates on a unique level, unlike most of the others, which are degenerate. The value $N = 23$ is just sufficient to pick out the desired pathway while suppressing all other pathways.

phase signature as the cogwheel phases are advanced. We call these *degenerate pathways*. It would be impossible to process the 23 individual transients in order to separate the degenerate signals. This compression of information does not matter since we are only interested in signals generated by the single nondegenerate pathway $\{0, +3, +1, -1\}$. The multiple degeneracy of many unwanted pathways comprises a time saving in the cogwheel approach. In the conventional nested cycle approach, the degeneracy of unwanted pathways is more limited.

EXPERIMENTAL DEMONSTRATION

The cogwheel phase cycle COG23$(+3, 0, -1; -11)$ is demonstrated experimentally in Fig. 3. This figure shows two-dimensional 3Q-MAS ^{87}Rb ($I = 3/2$) spectra of powdered $RbNO_3$, obtained using the FAM-RIACT-FAM pulse sequence described in Ref. (*11*). Figure 3a shows the result of applying the conventional 35-step nested phase cycle, repeated 3 times, so that 105 transients were acquired for each t_1 increment; Fig. 3b shows the result of the 23-step cogwheel phase cycle, repeated 4 times, so that 92 transients were acquired for each t_1 increment. Other experimental parameters are given in the caption. Both spectra are of good quality, with good resolution of the three inequivalent ^{87}Rb sites, and the signal-to-noise ratios conform to the expected ratio of $\sqrt{105/92} = 1.06$.

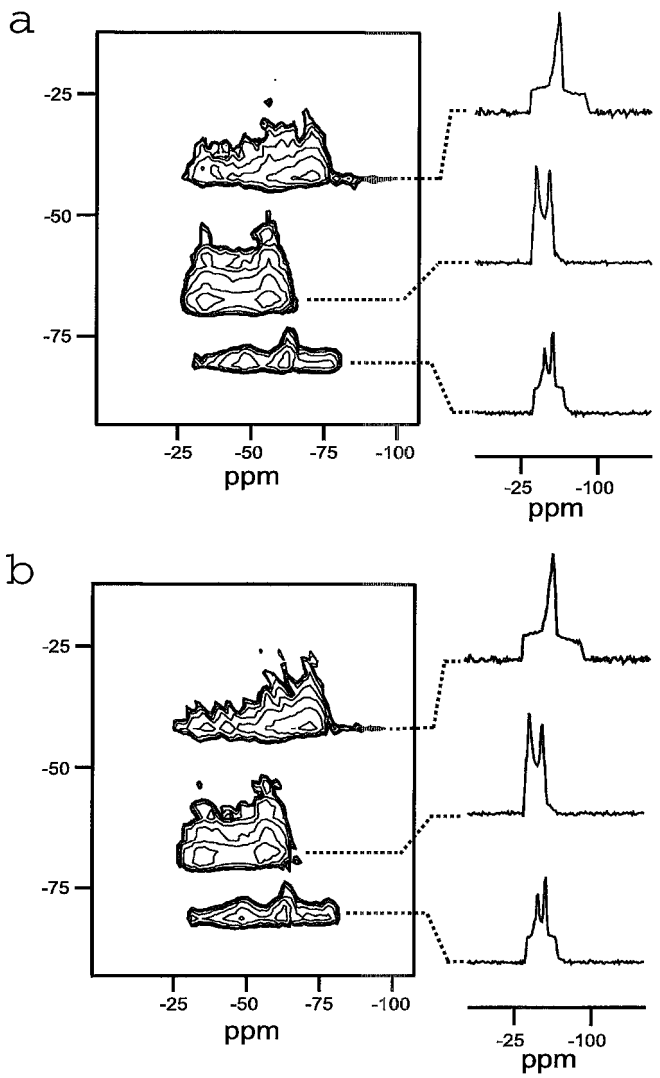

FIG. 3. Experimental ^{87}Rb 3Q-MAS of $RbNO_3$, obtained at 4.7 T using a Chemagnetics 4 mm MAS probe and an Infinity-200 spectrometer. The acquisition dimension is horizontal and the evolution dimension is vertical. The sample spinning frequency was 10 kHz. The FAM-RIACT-FAM sequence was used in both cases (*11*). The nutation frequency of the ^{87}Rb central transition was 70 and 20 kHz, for the hard and soft pulses, respectively (see the two indicated rf levels in Fig. 1). Each FAM interval consisted of a repetition of four elements, pulse–delay–pulse–delay, where each element lasted 1 μs, and the pulse phases differed by π. The first FAM interval consisted of 25 loops (corresponding to one rotor period), while the second FAM interval consisted of 3 loops. The strong rf field during the RIACT sequence lasted 25 μs (one quarter of a rotor period); 128 t_1 increments were used, with steps in t_1 of 20 μs. A waiting interval of 1 s was allowed between acquired transients: (a) 2D spectrum using 4 repetitions of the 23-step cogwheel phase cycle COG23$(+3, 0, -1; -11)$; (b) 2D spectrum using 3 repetitions of the 35-step nested phase cycle (Eq. [8] and Eq. [10]). Both spectra show three resolved ^{87}Rb sites, with comparable signal-to-noise ratio, as shown in the displayed anisotropic slices.

PREDICTION OF COGWHEEL PARAMETERS

In some cases, it is possible to predict the parameters of minimal cogwheel cycles without performing numerical searches. If the single pathway $\boldsymbol{p}^0 = \{0, p^0_{AB}, p^0_{BC}, -1\}$ is to be selected, and all other pathways of the form $\boldsymbol{p} = \{0, p_{AB}, p_{BC}, -1\}$ are to be rejected, and if the maximum coherence order supported by the spin system is $p_{\max}$, then the optimal cogwheel parameters are predicted to be

$$\begin{aligned} N &= \left(p_{\max} + 1 + \left|p^0_{AB}\right|\right)\left(p_{\max} + 1 + \left|p^0_{BC}\right|\right) - 4\left|p^0_{AB}\, p^0_{BC}\right| \\ \Delta\nu_{AB} &= \left(\operatorname{sign} p^0_{AB}\right)\left(p_{\max} + 1 - \left|p^0_{BC}\right|\right) \\ \Delta\nu_{BC} &= \left(\operatorname{sign} p^0_{BC}\right)\left(p_{\max} + 1 - \left|p^0_{AB}\right|\right), \end{aligned} \qquad [22]$$

where sign$x$ is equal to 1 if $x \geq 0$ and is equal to -1 otherwise. This result applies in the case that the predicted values of $\Delta\nu_{AB}$ and $\Delta\nu_{AB}$ have no common prime factor. For example, for 3Q-MQMAS spectroscopy of isolated spin-3/2 systems, for which $\boldsymbol{p}^0 = \{0, +3, +1, -1\}$ and $p_{\max} = 3$, Eq. [22] leads to $\{N, \Delta\nu_{AB}, \Delta\nu_{BC}\} = \{23, 3, 1\}$, as depicted in Fig. 2.

A proof of Eq. [22], and further theorems for cogwheel phase cycles, will be given elsewhere.

FURTHER APPLICATIONS

We have also found advantageous cogwheel solutions for many other experiments. For example, consider the 5Q MAS NMR of isolated spins-5/2 in solids. In this case, the pathway $\{0, +5, +1, -1\}$ should be selected, with all other pathways having $|p| \leq 5$ rejected. The minimal nested phase cycle for this case has $11 \times 7 = 77$ steps. The minimal cogwheel cycles have 57 steps. One set of solutions has the parameters $\{N, \Delta\nu_{AB}, \Delta\nu_{BC}\} = \{57, +5, +1\}$, as predicted from Eq. [22]. An example is the cogwheel cycle COG57(0, 5, 6; 32).

Cogwheel phase cycles provide the most impressive gains in instrument time when there are multiple coherence transfer steps. Consider, for example, a TOSS (*18–20*) or PASS (*18, 21*) experiment on isolated spins-1/2 in a solid. Suppose that $5\,\pi$ pulses are used for preparing the transverse magnetization (*19–21*). In the presence of radio-frequency pulse imperfections, the phase cycling scheme should select the desirable signal pathway $\boldsymbol{p}^0 = \{0, +1, -1, +1, -1, +1, -1\}$ and reject all other pathways with coherence orders 0 or ± 1 between the π pulses. This may be achieved by nested phase cycling of all $5\,\pi$ pulses, in steps of $2\pi/3$, which requires $3^5 = 243$ steps (*19, 20*). A shorter nested phase cycle with the same selection properties is constructed by cycling the phase of the preparation pulse in steps of $2\pi/3$, and the phases of the second and fourth π pulses in steps of $2\pi/5$. This requires $3 \times 5 \times 5 = 75$ steps. A further decrease in experiment time is accomplished by using the 11-step cogwheel cycle

$$\begin{aligned} \phi^{(m)}_{\text{prep}} &= \phi^{(m)}_2 = \phi^{(m)}_4 = \phi^{(m)}_{\text{dig}} = 0 \\ \phi^{(m)}_1 &= \phi^{(m)}_3 = \phi^{(m)}_5 = \frac{2\pi}{11} m \\ \phi^{(m)}_{\text{rec}} &= 6 \times \frac{2\pi}{11} m, \end{aligned}$$

where $m = 0, 1 \ldots 10$, ϕ_{prep} is the phase of the preparation pulse (for example, a cross-polarization field), and $\phi_1 \ldots \phi_5$ are the phases of the π pulses. The notation for the cycle above is COG11(0, 1, 0, 1, 0, 1; 6). This cogwheel cycle accomplishes the same pathway selection as the 243-step nested cycle, in only 4% of the experimental time.

In general, the selection of the repeated echo pathway $\boldsymbol{p}^0 = \{0, -1, +1, -1, +1 \ldots -1\}$ in a sequence of one preparation element followed by n refocussing pulses, where n is even, requires $5^{n/2}$ steps in the nested procedure but only $2n + 1$ steps in the cogwheel procedure. For example, the selection of the unique multiple-echo pathway generated by a sequence of 100 π pulses requires $5^{50} \cong 9 \times 10^{34}$ steps in the nested procedure but only 201 steps in cogwheel phase cycles such as COG201(0, 1, 0, 1, 0 . . . 1, 0; -100). Such time savings open up new experimental possibilities, for example in Carr–Purcell multiple echo experiments (*22*).

The cogwheel phase cycles described here select a single coherence transfer pathway, while rejecting all others. However, it is also possible to design cogwheel phase cycles which select multiple coherence transfer pathways, as required, for example, in pure absorption 2D spectroscopy (*3, 4, 23*). This topic is under investigation.

Even shorter phase cycles may be constructed if some of the feasible coherence transfer pathways are known to have a small amplitude and may be neglected. We have ignored this possibility in the discussion above.

Cogwheel phase cycling is also expected to provide a range of new possibilities in heteronuclear experiments. We also anticipate hybrid approaches in which cogwheel phase cycles are combined with nested phase cycles and/or pulsed magnetic field gradients (*24*).

CONCLUSIONS

Cogwheel phase cycles provide a new approach to the construction of phase cycles, and they can provide large savings in instrumental time, in some circumstances.

At the moment, it is not clear whether cogwheel phase cycles have any disadvantages over conventional phase cycles. Cogwheel cycles involving many steps may require more accurate radio-frequency phases than nested cycles (just as a long chain of meshing cogwheels may require more accurate machining than a set of independently-driven wheels). This is the subject of future research.

Some previous workers have independently investigated the possibility of generating shorter phase cycles. The authors are aware of an unpublished manuscript by Chingas, which may contain anticipations of some of the present results. In addition, McClung and co-workers have developed a method for discovering redundancies in the standard phase cycles and have suggested shorter cycles for some experiments (*25*).

ACKNOWLEDGMENTS

We thank Marina Carravetta for discussions and Ole Johannessen for instrumental support. C.E.H. has received support from the Marie Curie Fellowship Program (Grant HPMF-CT-1999-00199).

Thanks to Norbert Mueller for printing some additional Cogwheel solutions.

REFERENCES

1. G. Bodenhausen, H. Kogler, and R. R. Ernst, *J. Magn. Reson.* **58,** 370–388 (1984).

2. A. D. Bain, *J. Magn. Reson.* **56,** 418–427 (1984).

3. R. R. Ernst, G. Bodenhausen, and A. Wokaun, "Principles of Nuclear Magnetic Resonance in One and Two Dimensions," Clarendon Press, Oxford (1987).

4. M. H. Levitt, "Spin Dynamics. Basics of Nuclear Magnetic Resonance," Wiley, Chichester, UK (2001).

5. L. Frydman and J. S. Harwood, *J. Am. Chem. Soc.* **117,** 5367–5368 (1995).

6. G. Wu, D. Rovnyak, and R. G. Griffin, *J. Am. Chem. Soc.* **118,** 9326–9332 (1996).

7. A. P. M. Kentgens and R. Verhagen, *Chem. Phys. Lett.* **300,** 435–443 (1999).

8. P. K. Madhu, A. Goldbourt, L. Frydman, and S. Vega, *Chem. Phys. Lett.* **307,** 41–47 (1999).

9. T. Vosegaard, P. Florian, P. J. Grandinetti, and D. Massiot, *J. Magn. Reson.* **143,** 217–222 (2000).

10. H. T. Kwak, S. Prasad, Z. Yao, P. J. Grandinetti, J. R. Sachleben, and L. Emsley, *J. Magn. Reson.* **150,** 71–80 (2001).

11. P. K. Madhu and M. H. Levitt, *J. Magn. Reson.* **155,** 150–155 (2002).

12. M. Edén and M. H. Levitt, *J. Chem. Phys.* **111,** 1511–1519 (1999).

13. A. Brinkmann, M. Edén, and M. H. Levitt, *J. Chem. Phys.* **112,** 8539–8554 (2000).

14. X. Zhao, M. Edén, and M. H. Levitt, *Chem. Phys. Lett.* **342,** 353–361 (2001).

15. P. K. Madhu, X. Zhao, and M. H. Levitt, *Chem. Phys. Lett.* **346,** 142–148 (2001).

16. A. Brinkmann and M. H. Levitt, *J. Chem. Phys.* **115,** 357–384 (2001).

17. M. H. Levitt, *in* "Encyclopedia of Nuclear Magnetic Resonance," supplement, Wiley, New York (in press).

18. W. T. Dixon, *J. Chem. Phys.* **77,** 1800–1809 (1982).

19. Z. Song, O. N. Antzutkin, X. Feng, and M. H. Levitt, *Solid State Nucl. Magn. Reson.* **2,** 143–146 (1993).

20. O. N. Antzutkin, Z. Song, X. Feng, and M. H. Levitt, *J. Chem. Phys.* **100,** 130–140 (1994).

21. O. N. Antzutkin, S. C. Shekar, and M. H. Levitt, *J. Magn. Reson. A* **115,** 7–19 (1995).

22. R. Freeman, "Spin Choreography. Basic Steps in High Resolution NMR," Spektrum, Oxford (1997).

23. D. J. States, R. A. Haberkorn, and D. J. Ruben, *J. Magn. Reson.* **48,** 286–292 (1982).

24. A. Jerschow and N. Müller, *J. Magn. Reson.* **134,** 17–29 (1998).

25. J. Ollerenshaw and R. E. D. McClung, *J. Magn. Reson.* **143,** 255–265 (2000).

26. K. H. Lin, T. Charpentier, and A. Pines, *J. Magn. Reson.* **154,** 196–204 (2002).